International Journal of Chemical, Materials and Biomolecular Sciences
ISSN: 2415-6620
Vol:13, No:12, 2019

Tensile Properties of Aluminum Silicon Nickel Iron Vanadium High Entropy Alloys

Sefiu A. Bello, Nasirudeen K. Raji, Jeleel A. Adebisi, Sadiq A. Raji

***Abstract*—**Pure metals are not used in most cases for structural applications because of their limited properties. Presently, high entropy alloys (HEAs) are emerging by mixing comparative proportions of metals with the aim of maximizing the entropy leading to enhancement in structural and mechanical properties. Aluminum Silicon Nickel Iron Vanadium (AlSiNiFeV) alloy was developed using stir cast technique and analysed. Results obtained show that the alloy grade G0 contains 44 percentage by weight (wt%) Al, 32 wt% Si, 9 wt% Ni, 4 wt% Fe, 3 wt% V and 8 wt% for minor elements with tensile strength and elongation of 106 Nmm^{-2} and 2.68%, respectively. X-ray diffraction confirmed intermetallic compounds having hexagonal closed packed (HCP), orthorhombic and cubic structures in cubic dendritic matrix. This affirmed transformation from the cubic structures of elemental constituents of the HEAs to the precipitated structures of the intermetallic compounds. A maximum tensile strength of 188 Nmm^{-2} with 4% elongation was noticed at 10wt% of silica addition to the G0. An increase in tensile strength with an increment in silica content could be attributed to different phases and crystal geometries characterizing each HEA.

***Keywords*—**high entropy alloys, phases, model, tensile strength.

I. Introduction

APPLICATIONS of pure metals are limited due to failure of their properties in most cases to meet up with service requirements. Improvements in their properties are research focus over years either through alloying or composite systems [1]-[4], [7]. Both approaches employ greater proportion of metals as their matrix [13]. A small quantity of solute metal(s) or other materials is added to form alloy or metal matrix composite with consequent improvement in properties [10]. The pure metal as a system in a state possesses a certain amount of state variables (enthalpy, entropy and Gibbs' free energy). When the solute is added to the matrix melt, there is a change in the state variables, favouring formation of new structures with superior mechanical properties to those of the pure metals. That is, the improvement in the structural and mechanical properties is linked to differences in the entropy of the alloy from that of the pure metals. Initially, interaction of the matrix and solute is guided by Hume Ruthery's rule that predicts formation of solid solution when both matrix and solute metals have the same crystal structure, comparable atomic sizes and similar electronegativities [16], [9]. Surprisingly, recent findings have shown that enhancement in alloy properties is a function of variations in entropy of the alloy when compared with that of the pure metal. This implies that the higher the proportion of the solute atom, the higher is the entropy of the newly developed alloy system and the better is the alloy properties. This gives room for mixing metals of comparable sizes to produce a new class of the alloy system known as HEA [15]. The HEA is distinguished from conventional alloy as it accommodates at least five different metals [13] of the same or different crystal structures unlike the same crystal structure tradition which is the case for the conventional alloy [14].

Sefiu Bello is with the Kwara State University, Nigeria (e-mail: belloshaafiu@gmail.com).

II. Materials and Methods

Metallic cans, silica sand and ferrosilicon are the raw materials used in this study. Metals used were sourced from cans for various drinks packages, obtained from Waste Disposal Unit, Yaba, Lagos State. The silica sands were packed from playing ground inside Federal Industrial Institute of Research Oshodi (FIIRO), Lagos Nigeria and ferrosilicon powders were obtained from Lab-Trade, Taiwo, Ilorin. The planetary ball mill (model: LIMOGES 28A20 92) was used to refine the silica sand at Ceramics Department, FIIRO. The cans were transformed into molten form by heating the cans in a steel crucible using an oil-fired pit furnace as shown in Plate 1. The slag forming on the surface of the molten metal was carefully screamed off before pouring into green sand molds (prepared from silica sand, clay and water) whose cavities were patterned to a cylindrical shape. After solidification and cooling to room temperature, 2 kg of the cast ingot was re-melted at 800 ˚C. Additive powder mixture containing 1.5 kg silica and 0.5 kg of ferrosilicon was added to the metal melt, stirred and heated to 1000 ˚C before pouring into the mold whose cavities are replica of representative standard samples for tensile and structural tests. This represents the alloy grade G0. The remaining melt was cast into alloy ingots.

In the typical production of other alloys, 500 g cast ingot was re-melted at the same temperature and 10 g of silica sand powder (Sp) (2% of the cast ingot) was added to the melt, stirred while heating and finally poured into the molds. The alloy samples were removed from the molds after solidification and cooling to room temperature and classified as alloy grade G1. Alloy grades G_2, G_3, G_4 and G_5 were produced by a repetition of the same process except with a 2% increment in mass of Sp addition at each until a maximum of 50 g Sp (equal to 10% of the cast ingot) addition to the melt. This is the final alloy grade denoted as G5. The casting was carried out at Foundry Workshop, Yaba College of Technology, Akoka, Lagos, Nigeria. Three samples each of alloy grade were subjected to tensile tests using Universal Testing machine, model: Instron 3369 of 5 0kN capacity at Mechanical Testing Laboratory, Kwara State University

(KWASU), Malete, Nigeria. Each sample was analysed at room temperature of 18 ˚C and 50% relative humidity by loading gradually at a strain rate of 1.25 x $10^{-4}s^{-1}$ until sample fractured. Average values and standard deviation of the tensile properties were estimated. The standard deviation was inserted in the graph as the error bars. Elemental analysis known as spark test was carried out on rectangular samples of all alloy grade using ARL Optical Emission Spectrometer, model QuantoDesk AA83673 at Metallurgical and Materials Laboratory, University of Lagos, Nigeria. Before the spectrometric analysis, samples' surfaces were ground and polished using emery paper of different sizes (from coarse to fine) and polished cloth. Structural analysis was carried out with the aid of Philip X-ray diffractometer. Peaks were fitted using X'pert high score software and fractured sample surfaces were tracked morphologically with the use of ASPEX 3020 Scanning Electron Microscope at Microstructural Laboratory, KWASU.

Fig. 1 Materials and casting of HEA (a) Drink cans, (b) stirring of the alloy mix and green sand mold prior to pouring of the melt

III. Results and Discussion

A. Structural Properties

Alloy grades Go-G5 contain Al, Si, Ni, Fe and V in addition to Mg, Mn, Cu and Ti classified as minor elements because of their low composition summing up to less than 9% (Table I). The composition does not give room for an element to be the matrix or host as found in the conventional alloy. The developed alloys belong to the class of HEAs. Structurally, the alloy with the grade Go has dendritic aluminum with 4.0494 Å each of lattice parameter a, b and c; 90˚ for each of α, β, Y implying that the detected Al belongs to a cubic unit cell of volume 66.40 cm^3. Its density is 2.7 gcm^{-3}. It is located at 38.3845, 44.7174 and 65.0149˚ (2tetha) with closed packed planes indexed with (111), (200) and (220), respectively. The respective interplanar spacing is 2.338, 2.024 and 1.4310 Å. In addition, Al_3Ni_2 and $Al_{0.5}Fe_3Si_{0.5}$ and $Al_2Fe_3Si_4$ are intermetallic detected as other phases present in Go in addition to the dendritic Al. Al_3Ni_2 is a hexagonal crystal having 4.065, 4.065 and 4.906 Å for lattice parameters a, b and c with angles 90, 90 and 120˚, respectively. Therefore, c/a of the Al_3Ni_2 hexagonal crystal is 1.2069 which is different from 1.633 of the ideal hexagonal structure. Density of the crystal is 4.76 gcm^{-3} and its unit cell has a volume of 70.21 cm^3. Al_3Ni_2 appears at 44. 7174˚ having a closed packed plane indexed with $[11\bar{2}0]$ and interplanar spacing of 2.0280 Å. $Al_{0.5}Fe_3Si_{0.5}$ has a cubic structure with the lattice parameter 5.710 Å and angle 90˚ each. It appears at 44.7174˚ having plane (220) with 2.03 Å and 100% relative intensities and at 65.2259˚ with (400); interplanar spacing, 1.43030 Å and 12% relative intensity. $Al_2Fe_3Si_4$ is an orthorhombic crystal with 3.6687, 12.385 and 10.147 as the lattice parameters a, b and c; 90˚ each of α, β and Y, respectively. Its density is 4.81 gcm^{-3} and volume of its unit cell is 461.05 cm^{-3}. It appears at 38.3845˚ and 65.0149˚in a plane indexed with (043) and (117) with interplanar spacing, 2.2838 Å and 1.34002 Å, respectively (Fig. 3).

Atoms of detected phases at different positions around the Al grain boundaries and within the Al grains cause straining of the alloy either by compression or tension depending on their sizes and sizes of dendritic Al atoms. Presence of such straining effects in addition to differences in their crystal geometries of the phases may subject the alloy to high degree of disorder (increased entropy) and promote enhanced impingement/resistance to dislocation movement. Each of the phases creates disturbance in crystal equilibrium in fitting themselves in the Al lattice. The crystal disorder due to differences in their crystal structures is associated with low energy resulting in enhanced strengthening of the alloy via a fortified resistance to dislocation movement or dislocation impingement. Therefore, phases dominant in Go are Al, Al_3Ni_2 and $Al_{0.5}Fe_3Si_{0.5}$ and $Al_2Fe_3Si_4$. Silicon (Si) was not detected from XRD as a distinct element. This may be due to its limited solubility in Al, enhancing its tendency to react with Ni, Fe, Ti, V and Al to favour formation of the detected intermetallic compounds or phases. Limited solubility of Si in Al has been reported by different authors [8], [11].

TABLE I
Elemental Composition of the Alloy Grades Obtained from the Spectrometer

S/N	% Silica addition	Percentage elemental composition					
		Al	Si	Ni	Fe	V	Others
1	0	44.00	32.00	9.00	4.00	3.00	8.00
2	2	46.90	32.10	9.50	8.00	3.02	8.14
3	4	40.00	38.00	8.00	3.33	7.00	4.00
4	6	37.60	40.00	6.80	2.93	7.60	5.60
5	8	34.85	42.75	5.75	1.00	7.99	4.83
6	10	31.5	45.2	5.3	0	9.28	3.36

The dominant phases of Go are different from phases characterising the Al-Si and Al-Fe alloys. These affirm different interactions of the elements when their percentage compositions are comparable unlike what is observable with conventional alloys such Al-Fe and Al-Si systems. For instance, Al-Fe alloy containing 3wt% Fe (i.e. Al-3Fe) subjected to equal channel angular processing (ECAP) was reported to have Al dendrites with fine Al-Al6Fe eutectics as

dominant phases [6]. Also, Al, monoclinic $Al_{13}Fe_4$, orthorhombic Al6Fe, Fe and orthorhombic Al_5Fe_2 were confirmed as the phases present in Al-5Fe produced from High Pressure Torsion (HPT) [5]. For Al-Si alloy, Si has a limited solubility in Al and precipitates as eutectic during cooling at 578 ˚C and 12.6wt% Si. Due to extremely low solubility of Si (1.26wt%) in Al, Si exists as an elemental phase in Al rich α phase when Si is added to Al. However, Fe is added as an impurity to serve as an elemental linkage phase between Al and Si [8] promoting chemical reaction (instead of dissolution/solubility of Si in Al) to precipitate Al-Fe-Si phase as observed in this study through detection of $Al_{0.5}Fe_3Si_{0.5}$ and $Al_2Fe_3Si_4$. Evidence of Na, Mg, Ni, Sr and Ti up to a maximum of 0.05% as a modifier was reported in literature [8], [11], [12]. This is achieved by shifting Al rich α-Si eutectic to higher Si content by delaying precipitation of pro-eutectic Si with refinement of eutectic structure. Since Si contents of Go-G5 are higher than eutectic composition, they can also be regarded as hypereutectic Al-Si alloy in addition to HEA. Therefore, presence of primary or pro-eutectic Si is expected to be among phases of Go-G5. Its absence as disclosed earlier could also be attributed to higher proportion of additional elements such as Ni, Fe, V and others. Their high contents in the alloy expand their function beyond being a modifier but also a promoter of intermetallic formation which is evidenced by detection of Al_3Ni, $Al_{0.64}Ti_{0.36}$, $Al_{75}Fe_{15}Ni_{10}$, Al_2Ti and $Al_3Ti_{0.67}V_{0.33}$ (see Figs. 3, 4). $Al_{0.64}Ti_{0.36}$ is tetragonal having lattice properties a = 4.0296, b = 4.0296, c = 3.9561, α = β = Y = 90˚, density = 3.55 gcm^{-3} and volume = 64.24 cm^3, plane indexed with (202) and spacing 1.41120. Crystal structure of $Al_{75}Fe_{15}Ni_{10}$ is currently unknown. Al_2Ti is orthorhombic with lattice parameters and angles: a = 12.0944 Å; b = 3.9591 Å; c = 4.0315 Å; α = β = Y = 90˚. It has a plane indexed with (602) and a spacing of 1.42477 Å. $Al_3Ti_{0.67}V_{0.33}$ is a tetragonal crystal with lattice profiles of 3.8260, 3.8260 and 8.5210 with angle 90˚ each.

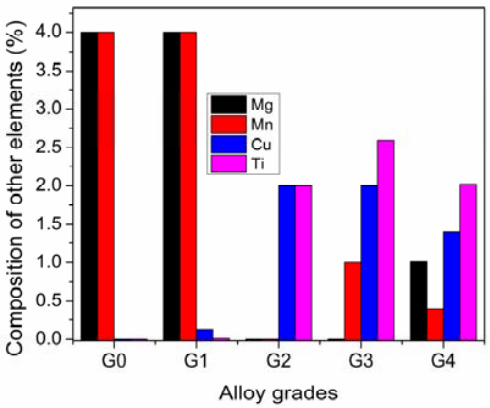

Fig. 2 Composition of other elements forming of HEA constituents

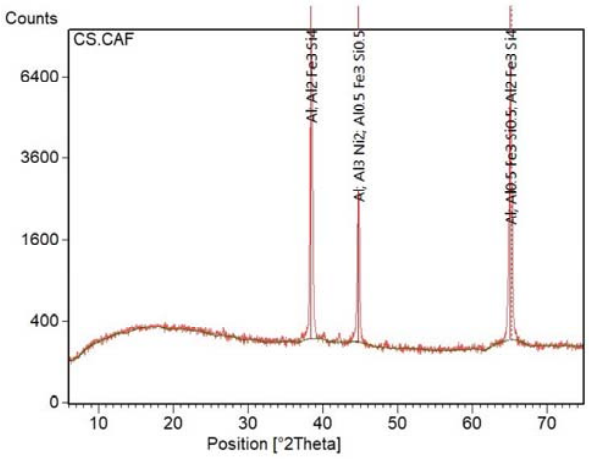

Fig. 3 X-Ray diffractogram of HEA containing no additional silica

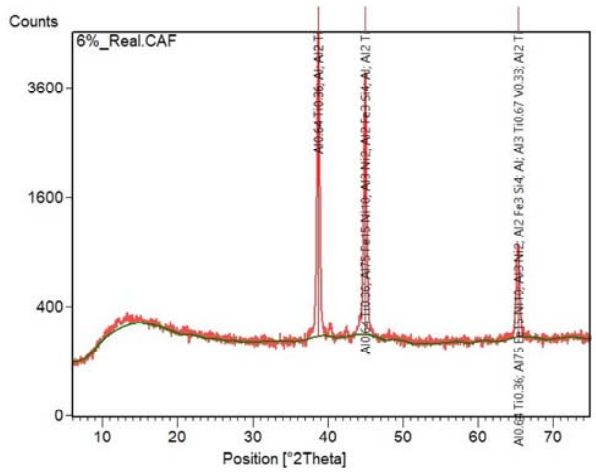

Fig. 4 X-Ray diffractogram of HEA containing 6wt% silica

Density and volume of $Al_3Ti_{0.67}V_{0.33}$ are 3.46 g/cm^3 and 124 cm^3, respectively. Due to presence of Al on all peaks, its proportion in Go seems greatest among other phases. Therefore, structure of the alloy grade Go can be described as having cubic matrix occupying hexagonal and orthorhombic structures. Similarly, G3 has cubic, tetragonal and orthorhombic matrix with hexagonal island. Under loading, deformation or stretching is expected to occur by slip in a closed packed plane and closed packed direction. For faced centre cubic matrix, it takes place in any of {111} planes and along any of <110> directions. Likewise, in orthorhombic structure; slip may occur in either (043) or (117) plane and (202) in tetragonal structures. This implies that the HEA G_3 has many slip systems that can give room for substantial plastic deformation with consequent high strength and ductility. Since elemental compositions of Go-G5 are different, degree of deformation of each of the HEAs varies depending on their phases and crystal structures (see Figs. 3, 4). Al, $Al_2Fe_3Si_4$, Al_3Ni_2, $Al_{0.5}Fe_3Si_{0.5}$ are the phases of Go, having the XRD profile in Fig. 3. Apart from aluminum, other phases of G3 (see Fig. 4) are completely different from those

of Go. Therefore, different phases are expected to be found in G1, G2, G4 and G5. This will lead to different responses of each of the AlSiNiFeV HEAs to mechanical loading. Since Al, Si and Ni are FCC crystals while Fe and V are BCC, it is worth noting that structures of the HEAs were produced or precipitated from transformation of FCC and BCC structures due to melting, solidification of all elements forming the HEAs.

B. Mechanical Properties

Tensile strength of HEA grade Go is 105.67 Nmm^{-2} with a tensile elongation of 2.68. Changes in response to mechanical loadings were observed after addition of silica sand to Go to modify its composition with intension of producing other grades of the HEAs as shown in Table I. At 2 wt% silica powder addition, new HEA produced designated with G_1 has a tensile strength of 107.15 Nmm^{-2} with the percentage elongation of 1.76. This implies a slight improvement in the tensile strength with a noticeable reduction in the elongation. Moreover, above 2 wt% of silica sand addition, a considerable increase in tensile strength was noticed (see Fig. 5). However, a shorter peak at 8wt% silica addition signifies lower tensile strength of the HEA grade G_4 than those of G_2 and G_3. The decrease could be attributable to defects such as shrinkage cavities within the G_4 sample. Although, the smaller tensile strength of G_4 might have been attached to excess or saturated silica particles, maximum tensile strength confirmed with G_5 at 10 wt% of silica particle addition negated the proposition of silica saturation. The increase in tensile strength could be linked to different phases that make up each alloy. In Go, Al, Al_3N_2, $Al_{0.5}Fe_3Si_{0.5}$ and $Al_2Fe_3Si_4$ share all XRD peaks in Fig. 3 implying that all phases exist in nearly equal proportions. Therefore, the HEA Go can be described as having FCC (Al), HCP (Al_3N_2), BCC ($Al_{0.5}Fe_3Si_{0.5}$) and orthorhombic ($Al_2Fe_3Si_4$) structures. Presence of Al in all peaks confirms its highest proportion among others. Therefore, its FCC structure is ranked as the matrix harboring other phases known as islands. Grain boundaries of the FCC matrix and island phases within the matrix are potential resistance to dislocations with consequent strengthening of the alloy Go. During tensile loading, deformation of the tested sample occurred in (043), (117) and basal plane (0001) along $[11\bar{2}0]$ in addition to (111) plane of the dendritic FCC Aluminum. Since slip occurs by dislocation movement, presence of crystals of different structures is a sign of impingement or resistance to dislocation movement. This implies that the islands phases strengthened the FCC matrix of Go by their resistance to the dislocation movement. This justifies higher tensile strength (105.67 Nmm^{-2}) of Go than 70 Nmm^{-2} of 99% Aluminum reported in [4].

At 6wt% of silica particle addition corresponding to G_3, $Al_{0.64}Ti_{0.36}$ (tetragonal) Al (FCC) and Al_2Ti (orthorhombic) appears on all peaks. This implies that all three phases are present in G3 in equal or nearly equal amounts. Therefore, G3 matrix can be considered as FCC, tetragonal and orthorhombic unlike Go that has only FCC matrix while Al_3N_2 (hexagonal), $Al_2Fe_3Si_4$ (orthorhombic) and $Al_{75}Fe_{15}Ni_{10}$ (unknown) appearing on one or two peaks are the island phases. This makes G3 a tri-phase HEA. Different crystal structures have varied degrees of close packing. For instance, degree of close packing in both hexagonal and orthorhombic structures is less than that in FCC and HCP structures. High shear stress is needed to cause slip in them or move dislocations. High shear stress requirement to cause movement of dislocation within G3 matrix implies that both hexagonal and orthorhombic structures enhance the strength of G3 but limitation in their slip has a consequence of a reduction in ductility of G3. But FCC structure of aluminum has numerous slip systems and is closely packed, implying that it has moderate strength and ductility. Island phases such as $Al_{75}Fe_{15}Ni_{10}$ and $Al_3Ti_{0.67}V_{0.33}$ are barriers which impinge dislocation movements in addition to grain boundaries of the matrix. Presence of the stiff and moderately strong phases forming the G3 matrix in addition to stiff island phases is a basis for higher tensile strength of G3 than Go having only FCC matrix. The same reason is proposed for the increase in the strength of HEA alloy as the wt% of silica particles addition increased. Decrease in the wt% of Aluminum (see Table I) favored formation of hard phases which improved the load bearing capacities of G1-G4 HEAs. Moreover, higher percentage elongation of G2-G5 might be attributed to an increase in number of slip systems of G2-G5 phases which gave room for prolong elongation of the alloys before fracture that succeeded the necking of the alloy.

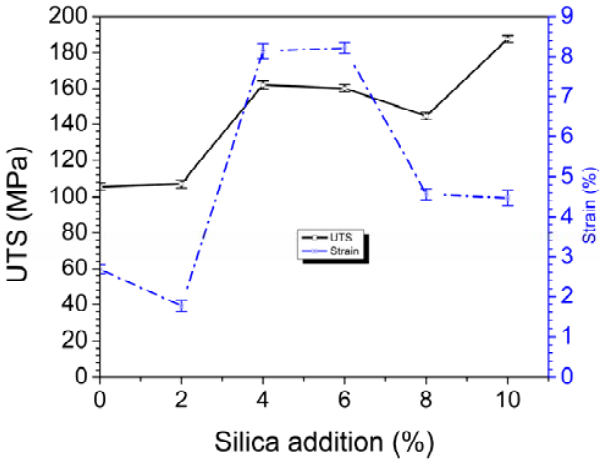

Fig. 5 Tensile properties of HEA at different silica particle additions

Apart from FCC that has substantial number of slip systems, addition of few numbers of slip systems of other phases would result in higher overall numbers of slip systems of the G_2-G_5 HEAs than that of G_0. The smaller percentage elongation of G1 than that of Go is assumed to be presence of hard phases in G_1 HEA. In addition, the increase in tensile strength can be attributed to an increase in entropy of the HEA due to numerous numbers of phase crystal structures of each of the alloys. Presence of additional phases such as Al_3Ni, $Al_{0.64}Ti_{0.36}$, $Al_{75}Fe_{15}Ni_{10}$, Al_2Ti and $Al_3Ti_{0.67}V_{0.33}$ increases degree of disorder in the matrix, implying higher resistance to dislocation movement. By considering the Gibbs' free energy formula in (1), it is observed that the increase in entropy (S)

causes a reduction in the value of the Gibbs free energy (G), where H and T are enthalpy and temperature. HEA will attain equilibrium when S increases to a level such that H is equal to TS. This can be achieved in the alloy by increasing number of islands phases in the matrix. Moreover, maximum tensile elongation confirmed with G_3 could be linked to ability of the phases to bear prolong stretching in addition to increasing load bearing capacity of the G_3. This could be linked to mixture of strong and ductile phases of G_3.

$$G = H - TS \quad (1)$$

IV. Conclusions

Based on experimental investigations, the following conclusions were made:

1. HEAs were developed from Al, Si, Ni, Fe and V using stir casting technique.
2. Phases of the alloys increased with a decrease in percentage by weight of aluminum.
3. Some face centred cubic structures of aluminum forming part of the raw materials retained after melting and solidification while BCC structures of Fe and V completely transformed into new structures.
4. HEAs of different tensile strengths were achieved with varied structures of phases of the alloys.
5. Tensile strength and percentage elongation increased with reductions and increments in Al and Si contents of the alloys.
6. Further studies are possible through combination of other elements including non-metals for developing new HEAs.

Acknowledgment

Authors appreciate technologists of Department of Materials Science and Engineering, Kwara State University, Malete, Nigeria and those of Department of Metallurgical Engineering, Yaba College of Technology, Nigeria for their assistance.

References

[1] Agunsoye, J. O., Bello, S. A., Talabi, S. I.… and Idegbekwu. T. E. (2015). *Recycled Aluminium Cans/Eggshell Composites: Evaluation of Mechanical and Wear Resistance Properties. Tribology in Industry,* 37 (1): 107-116.

[2] Aigbodion, V. S., Agunsoye, O. J., Edokpia, R. O. and Ezema, I. C. (2016). *Performance Analysis of a Connecting Rod Produced with Al-Cu-Mg/Bean Pod Ash Nanoparticles. Silicon.*

[3] Alaneme, K. K., Bodunrin, M. O. and Awe, A. A. (2016). *Microstructure, mechanical and fracture properties of groundnut shell ash and silicon carbide dispersion strengthened aluminium matrix composites. Journal of King Saud University - Engineering Sciences,* in Press.

[4] Bello, S. A., Raheem, I. A. and Raji, N. K. (2017). *Study of tensile properties, fractography and morphology of aluminium (1xxx)/coconut shell micro particle composites. Journal of King Saud University - Engineering Sciences,* 29: 269-277.

[5] Cubero-Sesin, J. M. and Horita, Z. (2012). *Mechanical Properties and Microstructures of Al-Fe Alloys Processed by High-Pressure Torsion. Metallurgical and Materials Transactions A,* 43 (13): 5182-5192.

[6] Fuxiao, Y., Fang, L., Dazhi, Z. and Toth, L. S. (2014). *Microstructure and mechanical properties of Al-3Fe alloy processed by equal channel angular extrusion. IOP Conference Series: Materials Science and Engineering,* 63: 012079.

[7] Harichandran, R. and Selvakumar, N. (2016). *Effect of nano/micro B4C particles on the mechanical properties of aluminium metal matrix composites fabricated by ultrasonic cavitation-assisted solidification process. Archives of Civil and Mechanical Engineering,* 16 (1): 147-158.

[8] Juan, A. L. and George, V. V. (2009). *Using Microstructural Analysis to Solve Practical Problems. Techno-Notes, Buehler,* 5 (1).

[9] Mittemeijer, E. J. (2011). *Fundamentals of Materials Science_ The Microstructure–Property Relationship Using Metals as Model Systems* (1 ed.): Springer-Verlag Berlin Heidelberg.

[10] Mohamed, A. M. A., Samuel, F. H., Samuel, A. M., Doty, H. W. and Valtierra, S. (2008). *Influence of Tin Addition on the Microstructure and Mechanical Properties of Al-Si-Cu-Mg and Al-Si-Mg Casting Alloys. Metallurgical and Materials Transactions A,* 39 (3): 490-501.

[11] Mohammad, S., Laurentiu, N. and Anwarul, H. (2014). *Development of High-Strength and Highly Ductile Hypo-Eutectic Al-Si Alloys by Nano-Refining the Constituent Phases.* Paper presented at the TMS (The Minerals, Metals & Materials Society).

[12] Muhammadreza, Z. (2015). *Al-Si Cast Alloys -Microstructure and Mechanical Properties at Ambient and Elevated Temperature.* (Bachelor degree Bachelor degree), Jönköping University, Sweden. (No. 7, 2015)

[13] Peter, K. L. (2014). Radiation Behavior of High-Entropy Alloys for Advanced Reactors. USA: Nuclear Energy University Programme 1-121.

[14] Reza, A., Lara, A. and Robert, E. R.-H. (2009). *Physical Metallurgy Principles* (P. Daly Ed. 4th ed.). USA: Cengage Learning.

[15] Tsai, M.-H. and Yeh, J.-W. (2014). *High-Entropy Alloys: A Critical Review. Materials Research Letters,* 2 (3): 107-123.

[16] William, D. C., Jr. (2007). *Materials Science and Engineering an Introduction* (7th edition). United State of American: John Wiley & Sons, Inc.